Mon. Not. R. Astron. Soc. **391,** 1874–1886 (2008) doi:10.1111/j.1365-2966.2008.13998.x

Near-infrared studies of V1280 Sco (Nova Scorpii 2007)

R. K. Das,[1⋆] D. P. K. Banerjee,[1⋆] N. M. Ashok[1⋆] and O. Chesneau[2⋆]

[1]*Astronomy and Astrophysics Division, Physical Research Laboratory, Navrangpura, Ahmedabad 380009, India*
[2]*UMR 6525 H. Fizeau, Univ. Nice Sophia Antipolis, CNRS, Observatoire de la Côte d'Azur, Av. Copernic, F-06130 Grasse, France*

Accepted 2008 September 23. Received 2008 August 13; in original form 2008 February 6

ABSTRACT

We present spectroscopic and photometric results of Nova V1280 Sco which were discovered in outburst in early 2007 February. The large number of spectra obtained of the object leads to one of the most extensive, near-infrared spectral studies of a classical nova. The spectra evolve from a P-Cygni phase to an emission-line phase and at a later stage is dominated by emission from the dust that formed in this nova. A detailed model is computed to identify and study characteristics of the spectral lines. Inferences from the model address the vexing question of which novae have the ability to form dust. It is demonstrated, and strikingly corroborated with observations, that the presence of lines in the early spectra of low-ionization species like Na and Mg – indicative of low-temperature conditions – appears to be reliable indicators that dust will form in the ejecta. It is theoretically expected that mass loss during a nova outburst is a sustained process. Spectroscopic evidence for such a sustained mass loss, obtained by tracing the evolution of a P-Cygni feature in the Brackett γ line, is presented here allowing a lower limit of 25–27 d to be set for the mass-loss duration. Photometric data recording the novas extended 12 d climb to peak brightness after discovery are used to establish an early fireball expansion and also show that the ejection began well before maximum brightness. The *JHK* light curves indicate the nova had a fairly strong second outburst ∼100 d after the first.

Key words: line: identification – techniques: spectroscopic – stars: individual: V1280 Sco – novae, cataclysmic variables.

1 INTRODUCTION

Nova V1280 Sco was discovered on 2007 February 4.8 independently by Sakurai & Nakamura (2007), within a short time of each other, with a reported visual magnitude in the range 9.4–9.9. The nova brightened quickly to its maximum in visual light on February 16.19 ($m_{\rm vmax} = 3.79$, Munari et al. 2007) to become one of the brightest novae in recent times (Schmeer 2007); V1500 Cyg in 1975 had a $m_{\rm vmax} = 2.0$ and nova V382 Vel 1999 had $m_{\rm vmax} = 2.5$. V1280 Sco has been observed in different wavelength regimes since its discovery. Early stage pre-maxima spectra was described by Munari et al. (2007) and Naito & Narusawa (2007) in the visible region and by Rudy (2007) and Rudy, Lynch & Russell (2007) in the infrared (IR). The early spectrum was dominated by absorption lines of hydrogen, neutral nitrogen and carbon, and displayed deep P-Cygni profiles. After passing the maxima, the spectrum turned to that typically shown by a classical nova; the lines started appearing in emission which included strong emission lines of Ca II H&K, the hydrogen Balmer series, the Na I D doublet and Fe II 42, 49 and 74 in visible region (Buil 2007; Munari et al. 2007). Early near-IR spectra by Das, Ashok & Banerjee (2007a) reported the presence of H I Brackett and Paschen lines and several strong C I lines. No X-ray detection was reported from the source from *RXTE* and *SWIFT* observations, respectively (Osborne et al. 2007; Swank 2007).

The nova has an interesting light curve with the possibility of more than one outburst. After passing the maxima, a smooth and slow decline followed. This was interrupted, about 24 d after discovery, by the formation of dust which was evidenced from the sharp decline in visible light curve and a rise in the IR continuum (Das, Ashok & Banerjee 2007b). The dust shell has been directly detected by interferometric techniques and its subsequent spatial expansion has also been tracked (Chesneau et al. 2008). Apart from providing the first direct detection of a dust shell around a classical nova, the Chesneau et al. (2008) study emphasizes the important, emerging role of interferometry in the study of dust formation and dust properties in novae. We present here spectroscopic and photometric results based on observations between 14 and 125 d after the discovery. A large number of spectra were recorded, sampling the novas evolution at regular intervals, thereby leading to one of the most comprehensive studies of a classical nova in the near-IR.

⋆E-mail: rkdas@prl.res.in (RKD); orion@prl.res.in (DPKB); ashok@prl.res.in (NMA); olivier.chesneau@ob-azur.fr (OC)

2 OBSERVATIONS

Observations of V1280 Sco in near-IR *JHK* were obtained at the Mt. Abu 1.2 m telescope. Near-IR *JHK* spectra presented here were obtained at similar dispersions of ∼9.75 Å pixel^{-1} in each of the *J*, *H*, *K* bands using the Near-Infrared Imager/Spectrometer with a 256 × 256 HgCdTe near-infrared camera multiobject spectrograph 3 (NICMOS3) array. Generally, a set of at least two spectra were taken with the object dithered to two positions along the slit. The spectra were extracted using IRAF and wavelength calibration was done using a combination of OH sky lines and telluric lines that register with the stellar spectra. Following the standard procedure, the nova spectra were then ratioed with the spectra of a comparison star (SAO 18 4301; spectral type A0V) from whose spectra the Hydrogen Paschen and Brackett absorption lines had been extrapolated out. The lack of a suitably bright standard star close to the nova, thereby leading to our choice SAO 18 4301, led to some difference in airmass between the nova and standard star observations. Thus, the ratioing process, while removing telluric features sufficiently well, does leave some residuals. This applies to regions where telluric absorption is strong (specifically, the 1.12 μm region in the *J* band and the 2 to 2.05 μm regions in the *K* band affected by atmospheric oxygen and carbon dioxide, respectively; we have thus excluded the latter *K*-band region from our spectra). Photometry in the *JHK* bands was done in photometric sky conditions using the imaging mode of the NICMOS3 array. Several frames, in five dithered positions offset typically by 20 arcsec, were obtained of both the nova and a selected standard star in each of the *J*, *H*, *K* filtres. Near-IR *JHK* magnitudes were then derived using IRAF tasks and following the regular procedure followed by us for photometric reduction (e.g. Banerjee & Ashok 2002). The log of the photometric observations and the derived *JHK* magnitudes, with typical errors in the range 0.01–0.03 mag, are given in Table 1.

Table 1. A log of the photometric observations of V1280 Sco. The date of outburst is taken to be 2007 February 4.854 UT.

Date 2007 (UT)	Days since outburst	Magnitudes *J*	*H*	*K*
February 19.972	15.118	3.33	3.05	2.78
February 25.962	21.108	3.58	3.09	2.77
February 27.991	23.137	4.00	3.63	3.79
March 01.992	25.138	4.71	4.27	4.21
March 03.996	27.142	5.42	4.43	3.55
March 05.991	29.137	6.23	4.88	3.62
March 07.995	31.141	6.68	5.09	3.78
March 10.986	34.132	6.82	5.15	3.93
March 13.979	37.125	7.21	5.45	4.03
March 27.950	51.096	7.62	5.51	3.88
March 28.971	52.117	7.72	5.61	3.83
March 31.981	55.128	8.25	5.98	4.13
April 01.972	56.118	8.29	6.04	4.19
April 02.981	57.127	8.25	5.97	4.01
April 03.988	58.134	8.32	6.04	3.90
April 05.975	60.121	8.27	6.08	4.20
April 08.982	63.128	8.27	6.05	4.05
April 15.963	70.109	8.10	5.90	3.91
April 18.953	73.099	7.89	5.78	3.93
April 26.871	81.017	8.84	6.58	4.52
April 30.890	85.04	8.85	6.70	4.62
May 02.920	87.066	8.69	6.38	4.36
May 03.922	88.068	9.10	6.71	4.49
May 04.899	89.045	9.33	6.95	4.81
May 05.920	90.066	9.06	6.79	4.63
May 06.898	91.044	8.64	6.38	4.26
May 08.910	93.056	9.13	6.77	4.62
May 15.798	99.944	8.81	6.41	4.11
May 22.800	106.946	7.26	4.94	3.06
May 30.811	114.957	7.36	5.16	3.25
June 02.809	117.955	7.73	5.47	3.23
June 05.791	120.937	8.08	5.73	3.67
June 07.772	122.918	8.23	5.78	3.58
June 10.773	125.919	8.15	5.77	3.81

3 RESULTS

3.1 Optical light curve

Before presenting the results proper, we estimate some of the useful parameters for V1280 Sco. The optical light curve is presented in Fig. 1. As seen, V1280 Sco is one of those few novae in which the light-curve data in the pre-maximum stage are well documented – two other novae, which come readily to mind, in which the pre-maximum ascent is similarly well studied and used to determine the onset of eruption are V1500 Cyg and PW Vul (Gehrz 1988, and references therein). After the maximum, the light curve declined steadily but was interrupted by dust formation around 24 d after discovery. We discuss in detail subsequently the dust formation phase and other specific phases in the light-curve evolution. For the present, we wish to determine t_2, the time for a decline of 2 mag in the visual band and note that the light curve indicates that dust formation had begun even before t_2 was reached. Hence to estimate t_2, we have extrapolated the light curve linearly in the post-maximum decline stage, as would have been the case had dust not formed at all, and thereby estimate t_2 to be approximately 21 d though slightly smaller values may also be supported. Using the maximum magnitude versus rate of decline (MMRD) relation of della Valle & Livio (1995), we determine the absolute magnitude of the nova to be $M_v = 7.88$ and obtain a distance estimate to the object $d = 1.25$ kpc for an assumed value of $A_v = 1.2$ as inferred from the extinction in the direction of V1280 Sco from the work of Marshall et al. (2006). It should be noted that the estimated value of d could be the subject to significant uncertainty.

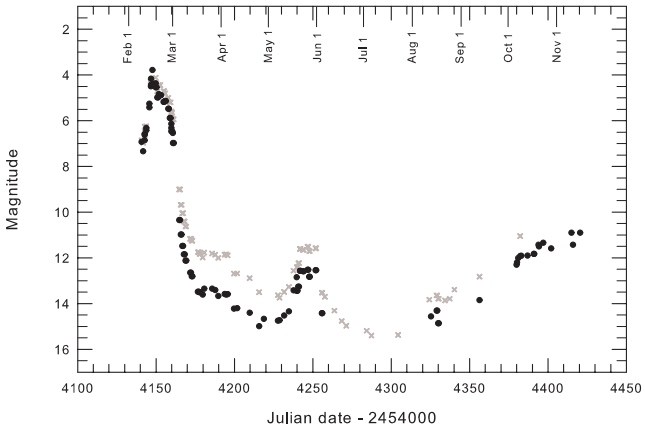

Figure 1. The *V* and R_c light curves (black circles and grey crosses, respectively) of V1280 Sco from data obtained from IAU circulars, VSNET alerts, VSOLJ and AFOEV data bases (Variable Stars Network, Japan; Variable Star Observers League, Japan and Association Francaise des Observateurs d'Etoiles Variables, France).

Table 2. A log of the spectroscopic observations of V1280 Sco. The date of outburst is taken to be 2007 February 4.854 UT.

Date 2007 (UT)	Days since outburst	Integration time (s)		
		J	*H*	*K*
February 18.981	14.127	10	10	10
February 20.006	15.152	10	10	10
February 24.990	20.136	10	10	10
February 25.997	21.143	10	10	10
February 26.968	22.114	10	8	10
February 27.972	23.118	10	8	10
March 01.964	25.110	10	15	15
March 03.961	27.107	20	15	20
March 04.961	28.107	20	20	20
March 05.965	29.111	45	20	20
March 06.965	30.111	40	30	30
March 07.951	31.097	60	20	20
March 10.963	34.109	90	45	30
March 13.950	37.096	100	40	30
March 28.928	52.074	150	60	30
March 31.920	55.066	300	45	30
April 02.902	57.048	300	40	30
April 05.905	60.051	350	60	40
April 18.891	73.037	500	60	30
April 27.870	82.016	500	60	45
May 04.954	89.100	450	60	45
May 06.833	90.979	500	45	30
May 22.865	107.011	300	40	20
May 30.854	114.999	350	40	30
June 05.758	120.904	400	90	30
June 08.836	123.982	350	60	40

This arises from errors in estimating t_2, A_v and also from the intrinsic errors associated with the MMRD relations.

Henden & Munari (2007) have made post-outburst astrometric and photometric measurements of the stars in the field around V1280 Sco and generated a photometric sequence to calibrate archival plates. Using SuperCosmos plates, a comparison was made between the magnitudes of stars therein with those of Henden & Munari (2007). A good consistency is found which allows us to conclude from the SuperCosmos data that no star is seen at the novas position down to *B* and *R* magnitudes of 20.3 and 19.3, respectively. A lower limit on the outburst amplitude *A* of the nova in the visual region can therefore be estimated to be in the range of ∼15.5–16 mag. Apart from the amplitude of the outburst being rather large, the compiled data of *A* versus t_2 for different novae (Warner 2008) show that V1280 Sco is very much an outlier. This, together with its long rise to maximum, early dust formation and the presence of a late time, secondary outburst makes the object somewhat unusual.

3.2 General characteristics of the *JHK* spectra

The log of observations for the spectroscopy is presented in Table 2. Instead of presenting all the spectra, we have rather chosen representative spectra sampling the observations at regular intervals which effectively convey the trend/behaviour of the spectral evolution. These *JHK* spectra are presented in Figs 2–4, respectively. The earliest spectra of February 18 show the lines to display P-Cygni structures with the absorption components considerably stronger than the emission components which are just beginning to appear. This is consistent with the near-IR spectroscopy of Rudy et al. (2007) between 14 and 16 February, wherein they report that the lines of hydrogen were in absorption; emission lines almost entirely absent and Pa β and Br α were just beginning to exhibit hints of emission and P-Cygni behaviour. By February 19, the emission components of the P-Cygni profiles become stronger than the absorption components and by February 24 the spectra become of pure emission type typical of a classical nova soon after maximum light. The emission lines remain at significant strength thereafter till the first week of March after which they lose contrast against the rising continuum from dust emission. The formation of dust in the ejecta at around the beginning of 2007 March can also be inferred – apart from it being seen as a drop in the visible light curve – from the change seen in the slope of the near-IR continuum. In each of the *JHK* bands, a rise in the continuum towards longer wavelengths is clearly seen. The development of this IR excess, attributable to dust, is seen till the end of our observations indicating that the freshly formed dust persists till then or is augmented by further episodes of dust formation. A detailed investigation of these aspects and analysis of the dust shell properties and kinematics is given in Chesneau et al. (2008).

3.3 Line identification and detailed study of spectral features

To facilitate a better understanding of the lines that contribute to a nova's spectrum, a model is developed based on local thermal equilibrium (LTE) considerations. It is likely that the model has limitations, based as it is on LTE assumptions which may not strictly prevail in a nova environment. Yet, we show that the model-generated spectra, greatly aids in a secure identification of the lines observed and also gives additional valuable insights. The synthetic spectrum is computed along similar lines as for nova V445 Pup in Ashok & Banerjee (2003) but is extended further here. The model spectra are generated by considering only those elements whose lines can be expected at discernible strength. Since nucleosynthesis calculations of elemental abundances in novae (Starrfield, Gehrz & Truran 1997; Jose & Hernanz 1998) show that H, He, C, O, N, Ne, Mg, Na, Al, Si, P and S are the elements with significant yields in novae ejecta, only these elements have been considered. For a particular element, we have first used the Saha ionization equation to calculate the fractional percentage of the species in different ionization stages (neutral plus higher ionized states). Subsequently, the Boltzman equation is applied to calculate the population of the upper level from which a transition of interest arises. The transitions of interest are essentially all the stronger lines of the above elements in the region of interest (1–2.5 μm) which was compiled from the Kurucz atomic line list and National Institute of Standards and Technology (NIST) line list. From the data base, for each line the statistical weight of the upper level of the transition, the energy difference between the upper energy level and the ground state and the transition probability is also noted. Given these parameters, and the partition functions (adopted from Aller 1963; Allen 1976), the population of the upper level for a particular transition – under LTE conditions – can then be derived from the Boltzman equation and the line strength can subsequently be calculated knowing the transition probability. For simplicity, we assume that the shape of each line can be reasonably represented by a Gaussian whose strength is known from the computed line strength and whose width can be adjusted to match that of the observed profiles. The co-addition of all such Gaussians – corresponding to all the lines – yields a model spectrum. In computing a model spectrum, values of certain parameters need to be assumed viz. the electron density N_e (needed in the ionization equation); the gas temperature *T* (needed

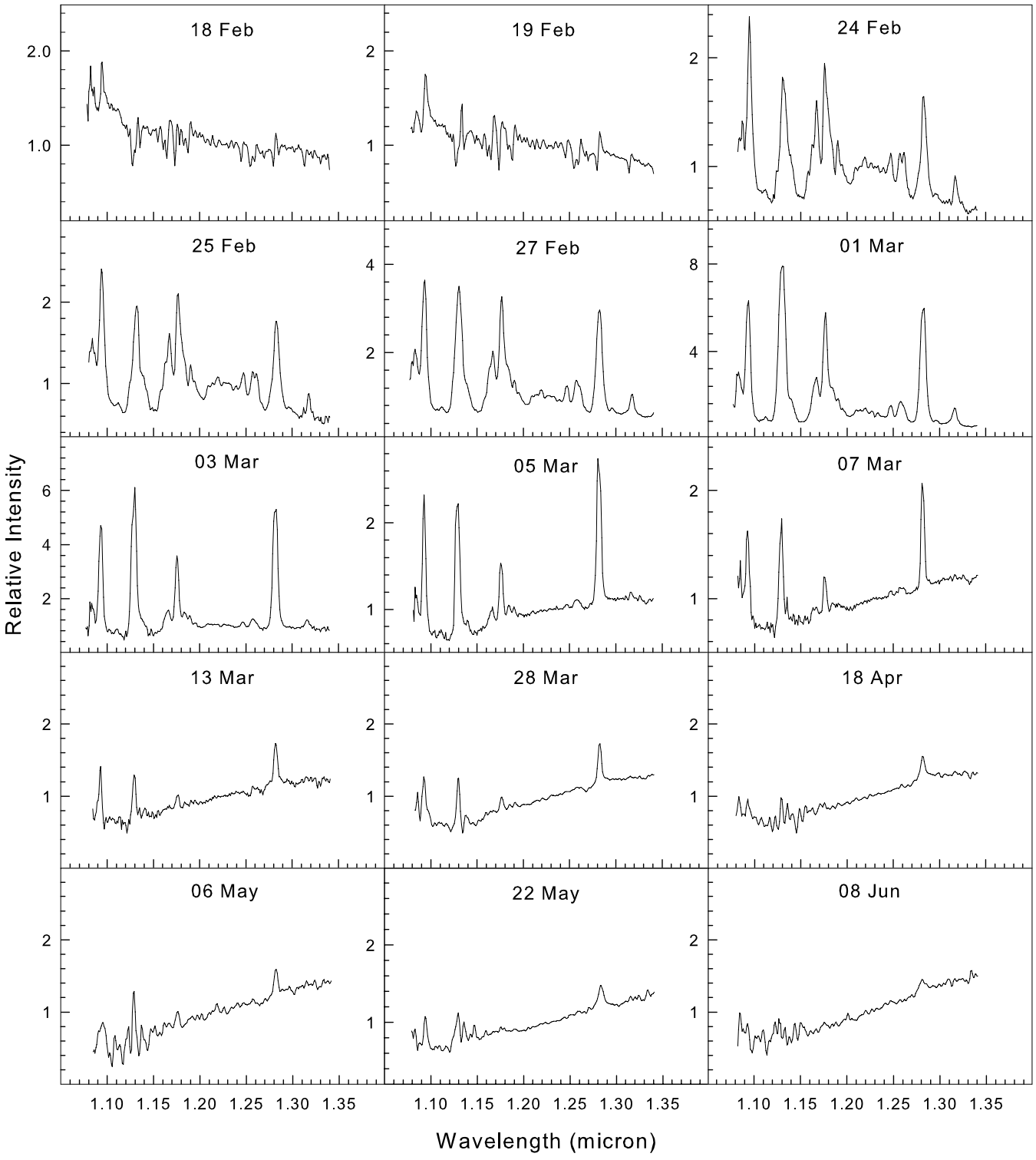

Figure 2. The *J*-band spectra of V1280 Sco on different days with the flux normalized to unity at 1.25 μm.

in both the Saha and Boltzmann equations) and the assumed abundances of the elements. We have considered typical values found in nova ejecta in the early stages viz. N_e in the range 10^9–10^{11} cm^{-3}, T ∼4000–10 000 K and abundances in line with those of CO noave given in Starrfield et al. (1997) and Jose & Hernanz (1998).

The computed spectrum is presented, overlaid with a representative observed spectrum for comparison, in Fig. 5 with the lines identified. The list of identified lines is given in Tables 3 and 4 (unidentified lines are marked as u.i). While most of the lines observed are known and identified from previous studies, there are a few subtle aspects influencing specific lines which are likely to have gone unnoted or whose significance could be under emphasized. A better understanding of these nuances emerge from our analysis. One such aspect is determining the relative contribution

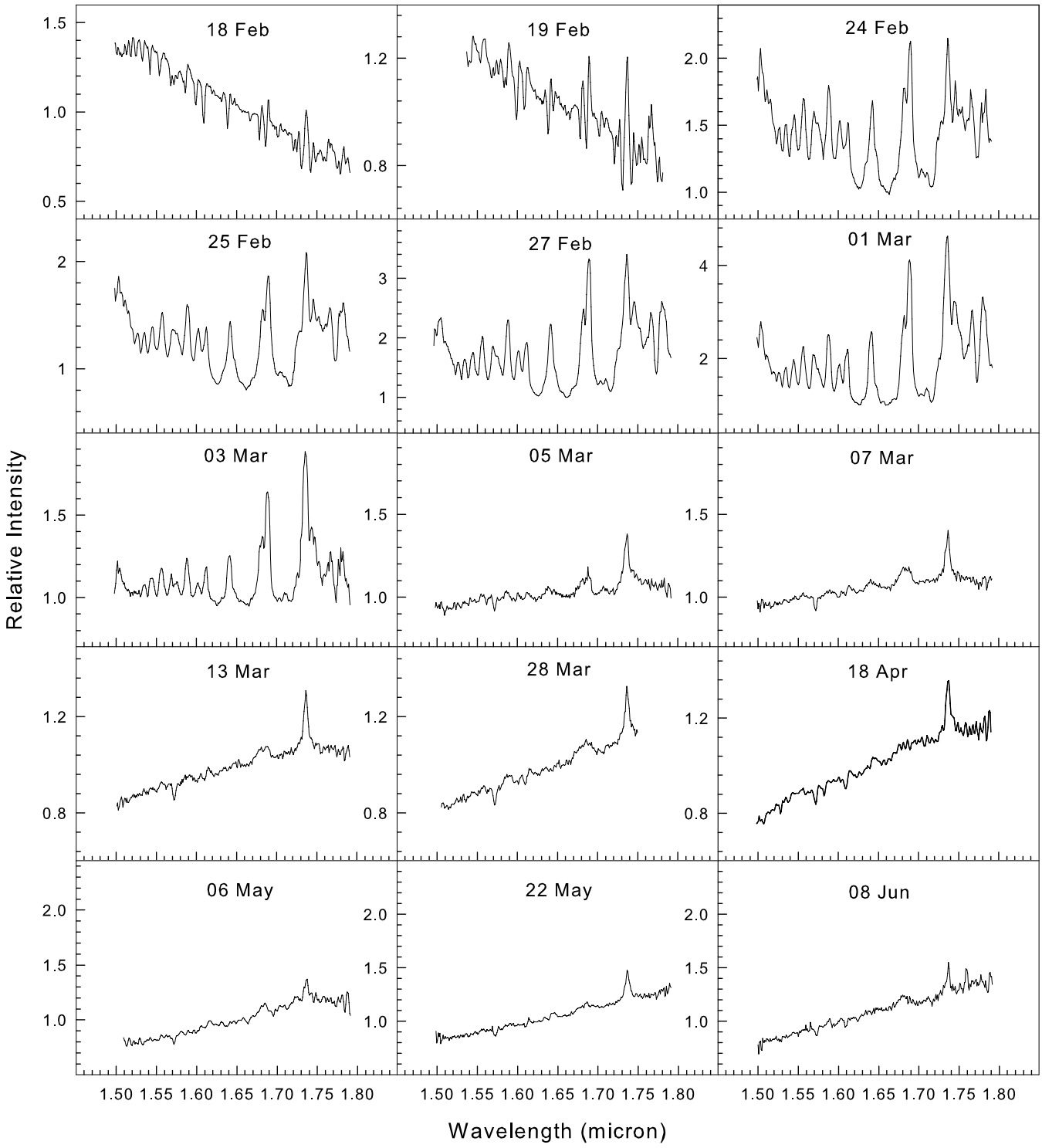

Figure 3. The *H*-band spectra of V1280 Sco on different days with the flux normalized to unity at 1.65 μm.

of different species to a particular spectral feature/line. Since in our model, trial spectra can be computed for one element at a time, the position and strength of all the lines of this element can be determined. Thus, it becomes clear to assess whether a particular line, at a particular wavelength, has one or more species is contributing to it. On the basis of such an analysis, we arrive at the following conclusions.

(i) In the *J* band, there is a Mg I line at 1.1828 μm in the wing of the strong Carbon lines at ∼1.1750 μm. This Mg I line, in case the nova emission lines are broad in general, may blend with the C I feature at 1.1750 μm giving the latter a broad redward wing. Alternatively, it may be seen as a distinct spectral feature as seen in V1419 Aql (Lynch et al. 1995) or in our observations on later days (e.g. the spectra of March 3 and 5). Establishing the identity of Mg lines unambiguously, and also that of Na lines, is important

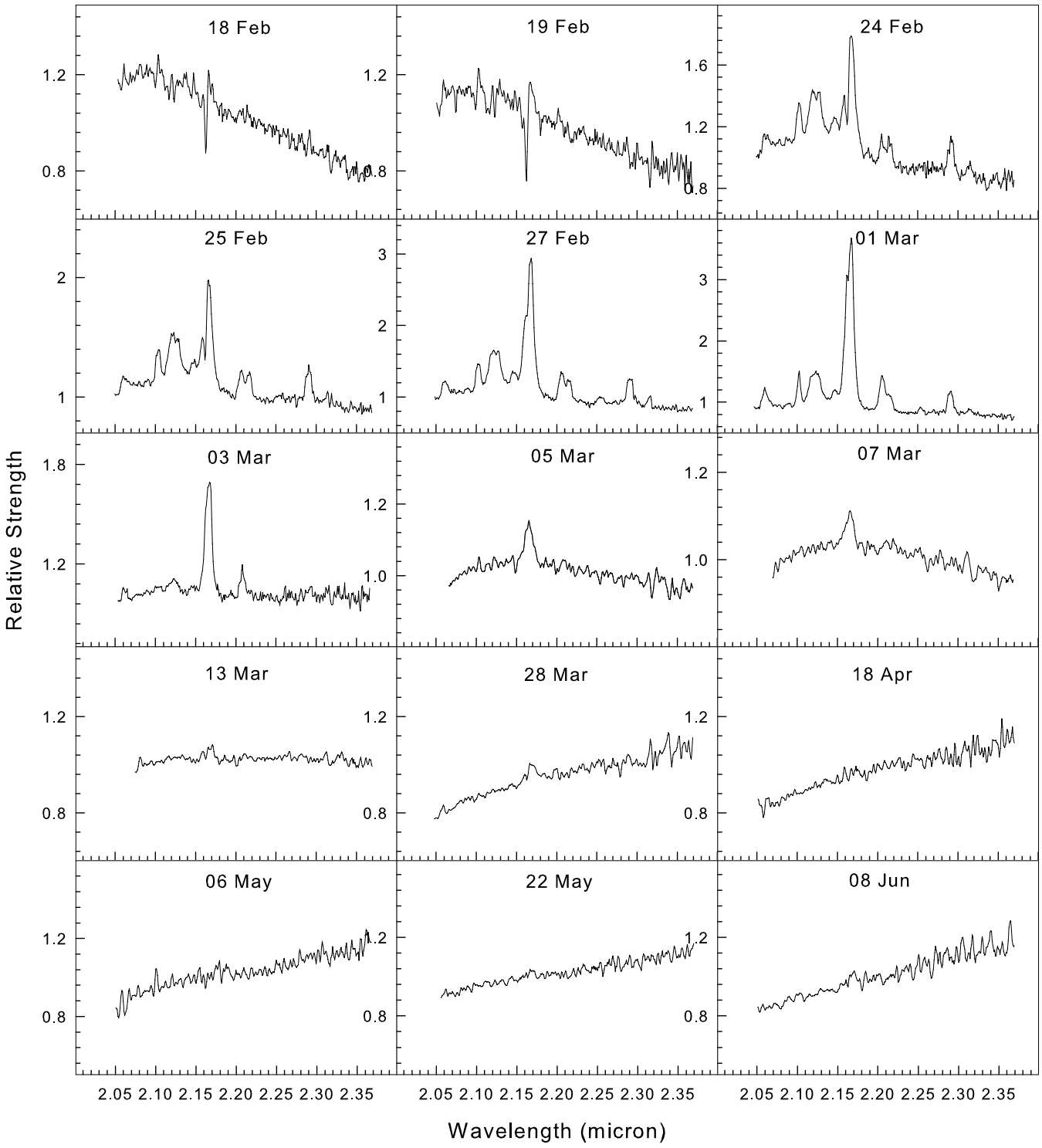

Figure 4. The *K*-band spectra of V1280 Sco on different days with the flux normalized to unity at 2.2 μm.

because we show subsequently that they are potential predictors of dust formation.

(ii) The region between 1.2 and 1.275 μm is a complex blend of a very large number of lines – principally those of N I and C I. This complex is routinely seen – always at low strength – in the early spectra of several nova including V2274 Cyg and V1419 Aql. Since our resolution in this region is higher than that of the V2274 Cyg and V1419 Aql spectra, we have tried to identify individual lines in the complex. Since most of the individual spectral features in this region are weak it is necessary to ensure their reliability. Thus, the data of February 5 were examined – since four, high signal-to-noise ratio (S/N) spectra are available for this date – and it was ensured that individual features repeat in all the four spectra. Subsequent line identification that followed, by comparing with the synthetic spectrum, is largely satisfactory but not completely so. The majority of the observed features are reproduced at the correct wavelengths

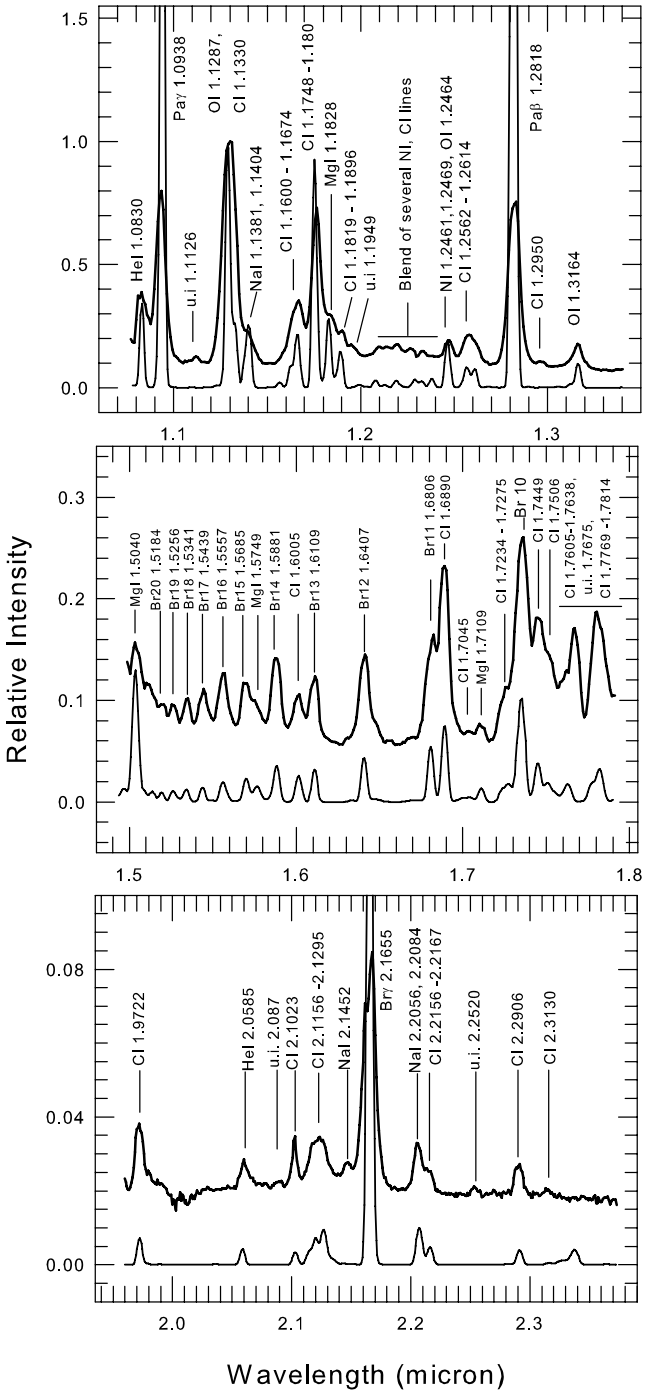

Figure 5. Line identification in the *J*, *H* and *K* bands shown from top to bottom panel, respectively. In each panel, the upper plot (darker shade) is the observed data of March 1 and the lower curve (lighter shade) is the synthetic spectrum (details in Section 3.3). More details on the lines are given in Tables 3 and 4. The observed spectrum was calibrated with the observed *JHK* magnitudes and normalized to unity with respect to the 1.1287 μm O I line whose peak strength is 5.6×10^{-15} W cm^{-2} μm^{-1}. The absorption features at ∼2.0 μm are residuals from improper telluric subtraction (discussed in Section 2).

Table 3. List of observed lines in the *JHK* spectra.

Wavelength (μm)	Species	Other contributing lines and remarks
1.0830	He I	
1.0938	Pa γ	
1.1126	u.i	Fe II?
1.1287	O I	
1.1330	C I	
1.1381	Na I	C I 1.1373
1.1404	Na I	C I 1.1415
1.1600−1.1674	C I	Strongest lines at 1.1653, 1.1659,1.166 96
1.1748−1.1800	C I	Strongest lines at 1.1748, 1.1753, 1.1755
1.1828	Mg I	
1.1819−1.1896	C I	Strongest lines at 1.1880, 1.1896
1.1949	u.i	
1.2074, 1.2095	N I	Blended with C I 1.2088
1.2140	u.i	
1.2187, 1.2204	N I	
1.2249, 1.2264	C I	
1.2329	N I	
1.2382	N I	
1.2461, 1.2469	N I	Blended with O I 1.2464
1.2562, 1.2569	C I	Blended with O I 1.2570
1.2601, 1.2614	C I	
1.2659	u.i	
1.2818	Pa β	
1.2950	C I	
1.3164	O I	
1.5040	Mg I	Blended with Mg I 1.5025,1.5048
1.5184	Br 20	
1.5256	Br 19	
1.5341	Br 18	
1.5439	Br 17	
1.5557	Br 16	
1.5685	Br 15	
1.5749	Mg I	blended with Mg I 1.5741,1.5766, C I 1.5784
1.5881	Br 14	blended with C I 1.5853
1.6005	C I	
1.6109	Br 13	
1.6335	C I	
1.6419	C I	
1.6407	Br 12	Blended with C I lines between 1.6335 and 1.6505
1.6806	Br 11	
1.6890	C I	
1.7045	C I	
1.7109	Mg I	
1.7200–1.7900	C I	Several C I lines in this region (see Fig. 5)
1.7362	Br 10	Affected by C I 1.7339 line
1.9722	C I	
2.0585	He I	
2.0870	u.i	
2.1023	C I	
2.1138	O I	This line may be present

in the synthetic spectrum except for the observed 1.2074, 1.2093 μm C I blend and the unidentified line at 1.2140 μm which are not. The N I 1.2461, 1.2569 μm feature is one of the stronger feature in the complex and while it has been attributed solely to N I by Rudy et al. (2003), it is likely that there is some contamination of this line with O I 1.2464 μm. In fact, the excess strength shown by this line in the synthetic spectrum is due to the contribution of the O I line in addition to the N I line. The contribution of O I, however, has made the line look too strong.

(iii) The blended feature comprising of the O I 1.1287 μm and C I 1.1330 μm lines shows considerable evolution with time. In the initial phase, for spectra between February 24 and March ∼5–7, the

Table 4. List of lines continued from Table 3.

Wavelength (μm)	Species	Other contributing lines/remarks
2.1156–2.1295	C I	Blend of several C I Lines strongest being 2.1156, 2.1191, 2.1211, 2.1260, 2.1295
2.1452	Na I?	
2.1655	Br γ	
2.2056	Na I	
2.2084	Na I	
2.2156–2.2167		Blend of C I lines at 2.2156, 2.2160, 2.2167
2.2520	u.i	
2.2906	C I	
2.3130	C I	

O I and C I lines contribute to the blend in comparable amounts. But with time the O I line begins to dominate possibly due to a increase in the Ly β flux with time as the central remnant becomes hotter. That Ly β fluorescence is certainly influencing the 1.1287 μm line can be inferred from its large relative strength compared to the continuum excited 1.3164 O I line. The 1.1287 μm O I–C I 1.1330 μm blended feature shows a broad red wing at 1.14 μm. There appears to be a strong case to believe, from the results of our synthetic spectrum, that Na I lines at 1.1381 and 1.1404 μm are responsible for this red wing. There are two carbon lines in this region which could contaminate the Na I lines but the effect of these C I lines is found to be very marginal from our model spectrum. It is also noted that the same Na I features are seen in the spectrum of V2274 Cen and identified by Rudy et al. (2003) as potentially arising from Na I.

(iv) In the *H* band, the recombination lines of the Brackett series are most prominent and readily identifiable. But the presence of a C I line at 1.6 μm, which could be mistaken as just another member of the Brackett series, should not be missed. If a recombination analysis of the Hydrogen lines is to be done, caution is needed in estimating line strengths of Br11 which can be severely blended with the strong C I feature at 1.6890 μm and Br10 at 1.7362 μm which is again blended with C I lines. Other Br lines, whose strengths are affected but to much lesser extent, are Br14 at 1.5881 μm (blended with C I 1.5853 μm and O I 1.5888 μm) thereby making it appear artificially stronger than Br12 contrary to what is expected in a Case B scenario; Br12 at 1.6407 μm is contaminated with several weak C I lines between 1.6335 and 1.6505 μm thereby giving Br12 a broad appearance on both the wings. A specifically interesting feature at 1.579 μm on the redward flank of Br15 (1.5701 μm) is due to Mg I; magnesium and sodium lines are discussed subsequently.

Before proceeding with other conclusions regarding line identification, it is relevant to point out at this stage that the early spectrum of V1280 Sco is very similar to that of the dust forming novae V2274 Cyg and V1419 Aql (Rudy et al. 2003; Lynch et al. 1995). A comparison of the 0.75–1.35 μm early spectra of these last two novae is given in fig. 8 of Rudy et al. (2003) to show the striking similarity in spectral features between them and examination of the *J*-band spectra shows that there is a one-to-one replication of spectral features in the case of V1280 Sco also. All three novae show a spectrum rich in H, C, O and N. Rudy et al. (2003) discuss in detail why it is not always easy to distinguish between CO and ONeMg novae based on near-IR spectroscopy alone. But they show that by considering several observational features together viz. the rate of decline, the expansion velocity, the formation of dust and the presence of C I lines that V2274 Cyg is strongly indicated to have a CO white dwarf (WD). By virtue of the same arguments, it would appear that V1280 Sco is also a CO nova. This is further supported by the classification of V1280 Sco as a Fe II nova based on its early optical spectrum (Munari et al. 2007) – Fe II novae are associated with explosions on CO white dwarfs (Williams 1992). It is intended to present results on three other novae which we have studied recently viz. V476 Scuti, V2615 Oph and V2575 Oph (Das, Banerjee & Ashok, in preparation). All three show rather similar spectra as V1280 Sco with prominent carbon lines and furthermore they all went on to form dust – a propensity shown preferentially by CO novae (Gehrz 1988; Starrfield et al. 1997). It is therefore tempting to think that a tentative hypothesis is emerging, subject to proper validation, that the characteristic near-IR spectrum shown by these nova is a hallmark of the CO class of novae. On a more definitive note, we hope to convincingly show that there are certain features in the spectrum of V1280 Sco that appear to be reliable, generic predictors whether dust will form in novae ejecta or not. A return is now made to a few other traits in the spectrum in Fig. 5 that deserve elaboration.

(v) Apart from the 1.1828 μm line, the other Mg I lines that we detect are those at 1.5040, 1.5749 and 1.7109 μm. The 1.5040 and 1.7109 μm are also suggested by Rudy et al. (2003) to be due to Mg I – we are convinced that this association is correct even if the 1.5040 μm line is at the edge of our observed spectral window. The feature at 1.5749 μm blending with the wings of Br 15 is certainly Mg I and may escape detection at lower resolutions where it could blend with lines of the Brackett series. The 1.5749 μm line can become quite strong, stronger than the adjacent Br lines as in the case of V2615 Oph (Das et al., in preparation) and a correlated increase in the strength between this line and other Mg I lines are also clearly seen in V2615 Oph. The identification of the Mg I lines is therefore felt to be secure. Regarding lines arising from Na, apart from those at ∼1.4 μm, the other lines that are definitively identified are those at 2.2056 and 2.2084 μm. These lines are known to occur in novae, for example, in V705 Cas (Evans et al. 1996). However, in the synthetic spectrum, we have trouble reproducing the 2.1045 μm feature – again associated with Na I (e.g. Evans et al. 1996) – at its observable strength. The identification is therefore uncertain.

(vi) The C I feature at ∼2.12 μm is actually a blend of several C I lines; the principal ones being at 2.1156, 2.1191, 2.1211, 2.1260 and 2.1295 μm. The superposition of these closely spaced lines gives the overall feature its unusually broad appearance.

(vii) There are a few weak lines which remain unidentified. One of these is the 1.1126 μm line which appears consistently in our spectra and which is often seen in the spectra of novae; Rudy et al. (2003) suggest its association with Fe II. However, our model shows that if this line is due to Fe II then several other lines of Fe II should also be seen – in the *H* band especially. Hence, we are doubtful about its origin. Similarly, a weak line is consistently seen at 2.2520 μm, prominently present too in the spectrum of V705 Cas (Evans et al. 1996), which eludes identification but which may be due to CO^+ (Dalgarno et al. 1997)

It may be noted that the Hydrogen line strengths are considerably overestimated in our model, particularly the stronger lines viz. Pa β and Br γ. One possibility, that could cause such behaviour, is that the assumption that LTE conditions prevail is a simplification. But this could be resolved if optical depth effects are considered. To illustrate this, we note that even if a non-LTE situation is considered,

as in Case B computations, then some difficulty may still persist in explaining the observed relative strengths of the H lines. For example, Pa β at 1.2818 μm is seen to be weaker than Pa γ at 1.0938 although Case B predicts the other way around (typically Pa β/Pa $\gamma = 1.6$ is expected). As we understand it, the optical depth in a line is proportional to the column density and the oscillator strength of the line. While the column density for all H lines will be the same, the oscillator strength decreases considerably for the weaker lines in a series (i.e. it is lower for Pa γ as compared to Pa β). This effectively causes the strength of Pa β to be reduced much more than for Pa γ. Rigorous modelling demonstrating this effect is given in Lynch et al. (2000) and an observed example is seen in nova N Sgr 2001 (Ashok et al. 2006), where Br γ is seen to be much weaker than later Br series lines like Br 10, 11 etc. In the present case, optical depth effects seem to be present, which if taken into account, is quite likely to reduce the strength of the stronger H lines and bring them in better agreement with the observed spectrum. In comparison to H, the optical depth in the lines of the other elements is expected to be significantly less – and hence their strengths remain unaffected – because of their considerably lower column densities (as a consequence of their lower abundances).

It was also found that use of a single temperature for the emitting gas fails to simultaneously reproduce the observed strengths of lines from all the elements. Though a complex interplay between the Saha and Boltzmann equations is involved, one of the principal reasons for this failure we believe, can be traced to the considerable diversity in ionization potentials (IP) of the elements contributing to the spectrum. The observed lines in the spectrum are from neutral species. If a higher temperature is considered (∼10 000 K), then the ionization equation indicates that elements like Na and Mg with low IPs of 5.139 and 7.646 eV, respectively, have a larger fraction of their atoms in higher stages of ionization and very few in the neutral state. Therefore, the lines from the neutral species of these elements are found to be extremely weak – the reduction in strength is compounded by the additional fact that they have low abundances. In comparison to Na and Mg, higher temperatures favour a relatively larger fraction of neutral species for H, C, N and O because of their significantly higher IPs (13.6, 11.26, 14.53 and 13.62 eV, respectively). On the other hand, instead of a high temperature, the use of only a single lower temperature (∼3500–4500 K) enhances the strength of Na and Mg lines to an unacceptable extent – they become too strong vis-a-vis lines of other elements.

It therefore becomes necessary to consider the possibility of temperature variation in the ejecta. We have adopted the simplest scenario viz. there exists a hot zone in the ejecta outside which lies a relatively cooler region. This involves invoking the least number of free parameters i.e. two temperature values for the hot and cool zone. Physically, the assumption of temperature variation in the nova shell does not appear unduly unreasonable – the formation of dust in V1280 Sco does indicate that there must be a cool region in the ejecta – though the temperature stratification is expected to be more complex than being characterized by just two temperature values. But our aim, as mentioned earlier, is to get a better qualitative idea of the characteristics of the emission lines seen. The model computation in Fig. 5 is therefore made on this basis using temperatures of 8300 and 3800 K for the hot and cool zones with their respective emitting volumes being in the ratio of ∼3:1. All other parameters are assumed to be the same in both zone viz. abundances, electron density etc. In this manner, we are able to reproduce reasonable agreement between observed and computed lines strengths of all elements except Hydrogen (which as explained earlier could be significantly affected by optical depth effects). The abundances that we used in Fig. 5, in terms of mass fractions, are 0.41, 0.21, 0.147, 0.096, 0.13, 0.0051 and 0.0010 for H, He, C, N, O, Ne and Na–Fe, respectively, which are reasonably consistent with that expected in CO novae (e.g. model CO4 of Jose & Hernanz 1998). However, we do not intend to stress that our model calculations determine elemental abundances in V1280 Sco or validate the assumption of LTE prevailing. But it appears that departure from LTE conditions may not be too severe in the early stages when the density in the ejecta is high. A conclusion that emerges from the analysis, and of which we feel fairly convinced, is the following. The presence of lines of particularly Na and also Mg, associated as they are with low excitation and ionization conditions, necessarily implies the existence of a cool zone. Such a zone is conducive for dust formation. In the coming section, using observational evidence for corroboration, we validate the claim that whenever these lines are seen it is also likely to be accompanied by dust formation in the nova.

3.4 Can we predict which novae will form dust from early IR spectra?

Considerable attention has been paid to understanding the dust formation process in novae and the fundamental physical conditions necessary for dust grain formation (Gehrz 1988; Evans 2001). It would appear that several parameters are involved in determining whether a nova has the ability to produce dust. Correlations between dust formation and parameters like ejection velocity and speed class have been examined but it is still not completely understood which novae will go on to form dust. Gehrz (1988) shows that for dust formation to take place efficiently, it is necessary that a sufficiently high particle density be available at the dust condensation point – the high density being necessary to enable the nucleation of grains to take place. It is also evident that low temperatures must prevail in the dust forming zone to enable dust to condense. Dust may fail to form in novae with low metal abundances. PW Vul and HR Del are the examples of dust-poor novae which probably had low CNO abundances – probably solar-like – whereas the novae that have formed thick dust shells have had an enrichment of CNO elements (Gehrz 1988, and references therein). Rudy et al. (2003) have found a significant correlation between novae in which carbon monoxide (CO) emission is seen and their dust producing capacity. They consider the known novae in which the first overtone of CO has been detected viz. V2274 Cyg, NQ Vul, V842 Cen, V705 Cas, V1419 Aql (Rudy et al. 2003; Ferland et al. 1979; Hyland & McGregor 1989; Wichmann et al. 1990; Lynch et al. 1995; Evans et al. 1996). All of these novae produced prolific amounts of dust. Rudy et al. (2003) comment that the association of dust with CO may not be totally unexpected, given that CO formation maybe a precursor for dust formation (Rawlings 1988; Evans et al. 1996) since CO emission could cool the regions sufficiently that dust formation can occur. Additionally, the low-temperature, high-density, metal-rich environment needed for CO production also favours the production of dust.

Among these physical parameters, the signature of a low-temperature condition can also be inferred from the presence of Na and Mg lines. We have therefore inspected the *JHK* spectra of these novae to see whether Na and Mg lines were present in their spectrum. In addition, since high densities in the ejecta seem a prerequisite for dust formation, only the early spectra were inspected because the density is expected to be high at this stage before expansion thins it. Beginning with V2274 Cyg, this object showed lines of Na I 1.1381, 1.1404, 2.2056, 2.2084 μm and the Mg I 1.5040 and 1.7109

μm lines are also detected (Rudy et al. 2003) in spectra taken 18 d after outburst. The 1.1828 and 1.5749 μm Mg I lines are not seen but that appears to be due to inadequate resolution in distinguishing them from nearby lines with which they could be blended (see Tables 3 and 4). In V1419 Aql, during the early stages, among the *JHK* spectra only the early *J*-band spectrum is available taken 18 d after maximum light – the Mg I 1.1828 line is clearly detected in it (Lynch et al. 1995). 1.6–2.2 μm spectra of NQ Vul were recorded by Ferland et al. (1979) 19 d after the outburst. The S/N in these spectra is low but the Na I 2.2056, 2.2084 μm features are clearly discerned and listed as observed features. V705 Cas was extensively studied by Evans et al. (1996) with *K*- and *L*-band spectra recorded at three epochs prior to strong dust formation in this nova which took place ∼62 d after outburst. V705 Cas is an archetypal example in which dust formation was accompanied by a drastic drop of ∼7 mag in the visual light curve. The *K*-band spectra of V705 Cas taken a day before maximum and 26.5 d after peak light very prominently show the lines of Na I 2.2056, 2.2084 μm, respectively, and also the line at 2.1045 μm which is attributed to Na I (Evans et al. 1996). In the case of V842 Cen, while 1–5 μm IR spectra have certainly been recorded (Hyland & McGregor 1989; Wichmann et al. 1990, 1991), we are unable to examine the *JHK* region of the spectra – to infer about the presence of specific Na I/Mg I lines – as they do not appear to be published. The published Hyland & McGregor (1989) spectra cover the 2.9–4.1 μm region emphasizing the polycyclic aromatic hydrocarbon features detected in this while the Wichmann et al. (1990) spectrum covers only the 2.27–2.43 μm region, i.e. the focus is on the CO first overtone emission seen in the object. However, Wichmann et al. (1991) do report that emission lines of Na I were seen, apart from other lines of H, He, C, O, N, in the 1–4 μm region. Thus, all these four dust forming novae had lines of Na I and/or Mg I in their spectra.

Apart from these novae, we were unable to locate early *JHK* spectra of other novae to increase the sample size to test our hypothesis. However, we have some unpublished data on V2615 Oph, V476 Scuti and V2575 Oph (Das et al., in preparation; preliminary results in Das, Ashok & Banerjee 2007a,b,c) – it may be noted that strong first overtone CO emission was observed in V2615 Oph (Das et al. 2007c). Preliminary results indicate all three novae formed dust – from sharp declines seen in their light curves accompanied by the buildup of an IR excess. Quite consistently, Na I and Mg I lines are seen in the spectra of these objects too. And finally, they are seen in the present case of V1280 Sco; though it must be noted that CO did not form in this nova and yet it formed dust. Thus, there appears to be an extremely good one-to-one correlation between the presence of Na I/Mg I lines and the dust forming potential of a nova. Their presence, in early IR spectra, could therefore predict dust formation. All of these novae appear to be rich in heavy elements. Abundance calculations show this for V842 Cen (Andrea, Drechsel & Starrfield 1994) while for the other novae, for which abundance calculations are unavailable, a metal-rich ejecta can be inferred indirectly from the prominent/strong lines of C, N, O seen in their *JHK* spectra (especially the lines of carbon). In essence, dust formation in novae can be expected when conditions of low temperatures and high densities are satisfied along with the possible prerequisite of an enhancement in heavy elements.

3.5 Evidence for sustained mass loss

Examination of the Br γ 2.1655 μm feature in the data of February 24, February 25, February 27 and March 01 (Fig. 4) shows that there appears to be an additional line on the blue wing of Br γ. However, we are not able to identify this feature with any known line and therefore looked for alternative reasons for its origin. As it turns out, it is caused by the continued presence of the absorption component of a P-Cygni feature that persists quite long after the outburst began – at least till March 01. To demonstrate this, a velocity plot of Br γ region is shown in Fig. 6 on different days. The earliest spectra of February show classic P-Cygni profiles. What may be noted, however, is that the position of the P-Cygni absorption component in the earliest spectra closely tracks the trough seen in the peak of the Br γ line at later stages (February 24 to March 01). The trough it may be seen, by splitting the peak/profile of the Br γ line into two components, creates the impression of an additional line being present which, however, is not the case. The profiles in Fig. 6 can instead be interpreted as follows. A P-Cygni profile arises in an outward accelerating wind and is a indicator of mass loss. The initial P-Cygni structure arises from mass loss during the rise to maximum or epochs close to it. As this matter moves away from the central remnant, the line profile associated with it is expected to become purely of emission type. However, if strong mass loss continues, then superposed on this emission component will be the P-Cygni component arising from the continuing mass loss. The addition of these two components, as can be visualized, can lead to the profiles of the observed shape in Fig. 6. In effect, Fig. 6 indicates that observational evidence is seen that mass loss continues from the nova up to 2007 March 1–3 i.e. it lasts for at least 25–27 d after the outburst began. This estimate for the duration of the mass loss ($T_{\rm ml}$) is likely to be a lower limit for the process of mass ejection could continue longer but at reduced mass-loss rates insufficient to create the necessary absorption column density to produce a discernible P-Cygni absorption component on the overall profile. Our finding gives direct observational evidence for sustained mass loss and a constraint on its duration.

A comparison could be made between theoretical estimates of $T_{\rm ml}$ and its observed value from the grid of nova models developed

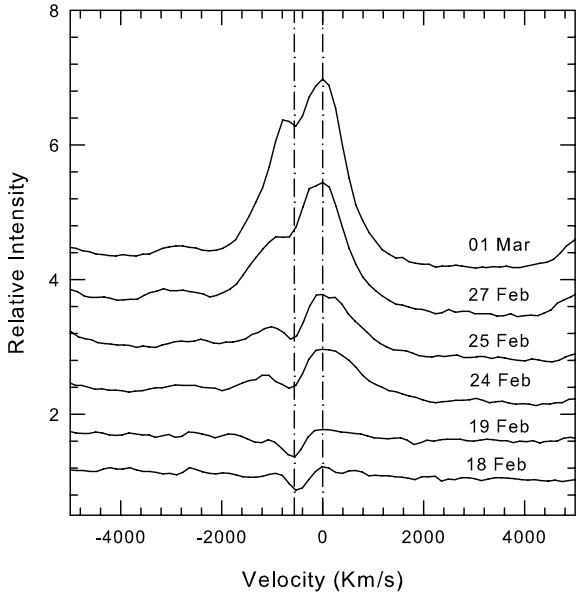

Figure 6. The time evolution of the Brackett γ2.1655 μm line showing the P-Cygni profile in the early stages with its absorption feature at $\sim -575\,{\rm km\,s^{-1}}$ blueward of the emission peak. An absorption component, coincident in wavelength with the P-Cygni absorption trough position, persists near the peak of the profile for several days indicating continuing mass loss (see the text of Section 3.5 for details).

by Prialnik & Kovetz (1995) and Yaron et al. (2005) providing numerical estimates for key quantities characterizing a nova outburst and properties of the ejecta. The different models are computed by varying the three basic and independent parameters that control a nova outburst viz the mass ($M_{\rm WD}$) and temperature of the WD and the mass accretion rate on the WD. One of the central time-scale parameters that they compute is $T_{\rm ml}$ which is shown to be of the order of t_3 (the time for a decline of 3 mag in the visual). The early formation of dust in V1280 Sco makes it difficult to estimate t_3. But if we proceed along the lines as our estimate of t_2, then t_3 should be in the range of 30–40 d. This seems to be satisfactorily consistent with the observed lower limit for the mass-loss time-scale of about 25–27 d. Together with the observed estimate of $T_{\rm ml}$ if the known outburst amplitude (A) and the expansion velocity ($V_{\rm exp}$) are also considered; then the grid of models can be used to estimate $M_{\rm WD}$ since A and $V_{\rm exp}$ are two other observable parameters predicted by the computations. In this context, it appears that a value of $M_{\rm WD}$ towards the higher end (1–1.25 $M_\odot$) may be supported. For example, one of the models with $M_{\rm WD} = 1.25\,M_\odot$ predicts a maximum velocity, average velocity, outburst amplitude and $T_{\rm ml}$ with values of 1230 km s^{-1}, 678 km s^{-1}, 14.3 mag and 22 d, respectively. This agrees reasonably with the A and $V_{\rm exp}$ values observed in V1280 Sco. However, this estimate of $M_{\rm WD}$ has to be viewed with due caution given the uncertainties in the observable quantities (we have only a lower limit on $T_{\rm ml}$ and A) in addition to the complicated behaviour of V1280 Sco which shows evidence for a second episode of significant mass loss about ∼100 d after the first outburst (see Section 3.7). It is also noted that a high WD mass would imply a ONeMg rather than a CO WD in this nova. But the IR spectrum definitely supports a CO classification. Thus, there could be a possible inconsistency here, which though not firmly established, could still be kept in mind.

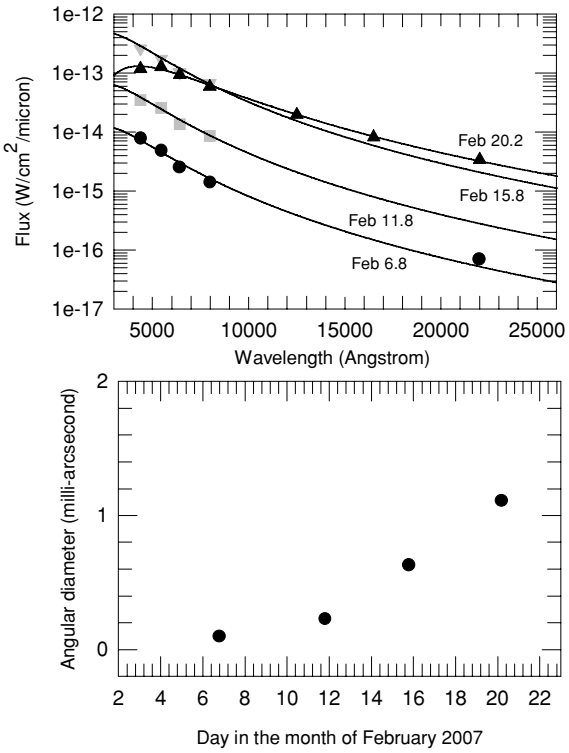

Figure 7. The top panel shows the observed SEDs on different dates fitted by blackbody fits after correcting for $A_v = 1.2$. The same blackbody temperature of 11 000 K is found to fit the data of February 5.8, 11.8 and 15.8 while for February 20.2, a temperature of 6750 K is used. The bottom panel shows the fireball expansion in V1280 Sco during pre-maximum and peak phase.

3.6 The initial fireball phase of V1280 Sco

V1280 Sco was first caught brightening on February 4.5 (Sakurai & Nakamura 2007) when it was found to be at 9.4–9.9 mag in the visible. Within the next ∼12 d, it brightened by nearly 5.8 mag to reach its maximum on February 16.2 at $V = 3.79$ (Munari et al. 2007). During this prolonged rise to maximum, extensive optical photometry of the object has been documented; not many novae have had been studied so well in the pre-maximum rise. Thus, the available data permit a study to be made of the early fireball expansion in the nova along similar lines as in PW Vul (Gehrz et al. 1988). In Fig. 7, using B, V, $R_{\rm c}$, $I_{\rm c}$ and *JHK* magnitudes, when available, reasonably good blackbody fits are obtained to the data thereby allowing a blackbody temperature $T_{\rm bb}$ to be derived. The blackbody temperatures obtained are consistent with the observation that the nova pseudosphere generally shows an A to F spectral type at outburst. The blackbody angular diameter $\theta_{\rm bb}$ in arcseconds is then obtained from (e.g. Ney & Hatfield 1978):

$$\theta_{\rm bb} = 2.0 \times 10^{11} (\lambda F_\lambda)_{\rm max}{}^{1/2} T_{\rm bb}{}^{-2}, \quad (1)$$

where $(\lambda F_\lambda)_{\rm max}$ is in W cm^{-2} and $T_{\rm bb}$ in Kelvin. The estimate of $\theta_{\rm bb}$ will always be a lower limit since it is applicable for a blackbody (Ney & Hatfield 1978; Gehrz et al. 1980). For a grey body, the actual angular size can be larger, since the right-hand side of equation (1) should then be divided by $\epsilon^{1/2}$, where ϵ the emissivity has a value less than unity for a grey body.

The angular diameter values are plotted in the lower panel of Fig. 7 and clearly show the expansion of the fireball. Though subject to some uncertainty, it would appear the expansion rate was marginally slower between February 6 to 12. But subsequently increased thereafter to ∼0.105 mas d^{-1}. This angular expansion rate is approximately a factor of 3 smaller than the mean rate of 0.35 mas d^{-1} determined from the interferometric data. As a consequence of this, values of parameters such as the angular size and the distance to the nova, when derived from the interferometric and fireball approach, will not match. For example, the March 23 interferometric data for which the shell size was well constrained, estimate its diameter to be 12–13 mas in comparison to ∼4.1 mas obtained by extrapolating the data in Fig. 7. Similarly, the Chesneau et al. (2008) results estimate a mean distance of 1.6 kpc for an adopted expansion velocity for the ejecta of 500 km s^{-1}; a similar choice of the expansion velocity will yield a distance three times larger using the fireball approach (since the distance is inversely proportional to the angular expansion rate). It is thus necessary to understand why this inconsistency arises between the two methods. The most likely source for this disagreement is that diameters derived from equation (1) are lower limits being applicable to a true blackbody which may not be the case here. The physical reasons which cause a departure in the nature of the emission from black to grey – as seems to be applicable here – are not entirely clear to us. Is it associated with clumpiness in the matter or the matter becoming optically thin? The fireball expansion data, extrapolated back to zero angular size, show that the onset of the eruption began around February ∼2.5, almost 2.35 d before the day of discovery and nearly 13.7 d before maximum light. A comparison could be made with V1500 Cyg and PW Vul, two other rare instances where the early fireball was documented sufficiently to enable estimating the onset of ejection. In both these novae, ejection began well before maximum light viz.

1.8 and 9 d for V1500 Cyg and PW Vul, respectively (Gehrz 1988, and references therein).

3.7 The *JHK* light curve of V1280 Sco

The *JHK* light curve is presented in Fig. 8 along with the visible light curve to enable a comparison. The first onset of dust around 12 d after maximum shows a sudden drop in the *V* magnitude. The contribution from the dust to the IR affects the near-IR bands whose magnitudes do not drop so sharply. The contribution to the *K* band is the greatest indicating the dust emission peaks at even longer wavelengths. That this is indeed so can be seen from the 0.5–13 μm SED plots of the object by Chesneau et al. (2008). These plots, though obtained at different epochs, show the SED to generally peak at 3 μm or slightly beyond indicating a blackbody temperature for the dust of ∼1000 K. Such peak temperatures for the dust are typically found in novae (Gehrz et al. 1988). Fig. 8 shows that on the whole, the *K*-band brightness remains quite high throughout our observations indicating the constant presence of dust during this time. The dust shell formed in V1280 Sco is not as optically thick as in novae like Nova Serpentis 1978 (Gehrz et al. 1980) or NQ Vul (Ney & Hatfield 1978) where the bulk of the entire emission at shorter wavelengths is absorbed and re-radiated by the dust into the IR. By fitting blackbody curves to our *JHK* magnitudes and the *N*-band fluxes of Chesneau et al. (2008), we estimate for V1280 Sco that the ratio of the maximum IR luminosity to the outburst luminosity (from data in Fig. 7) is ∼0.06. This ratio is found to be close to unity for optically thick novae like Nq Vul, LW Ser, etc. The fact that the IR luminosity is much less than the outburst luminosity, but that the dust is thought to cause the decline in the visual band, is suggestive of a clumpy shell. The clumps are individually optically thick, but do not cover the whole of the sky as seen from the nova. The decline in the *V* band could then occur when an optically thick clump of dust forms along the line of sight.

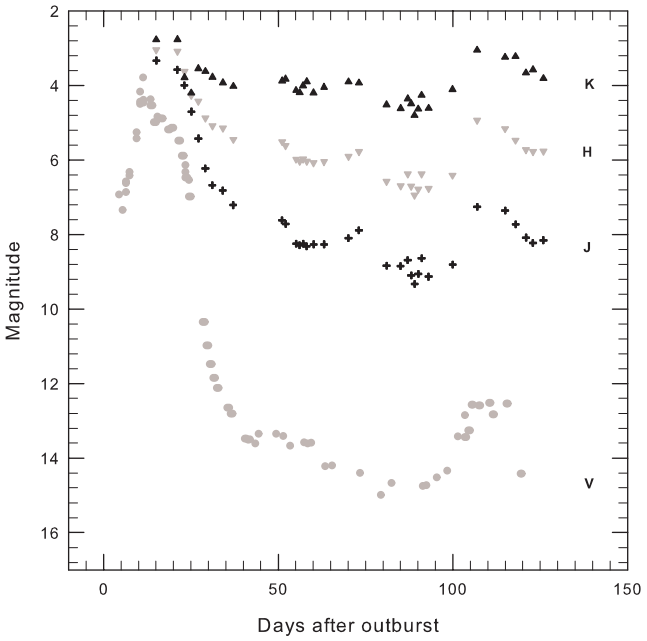

Figure 8. The *JHK* light curve of V1280 Sco from Mt. Abu observations overlaid on the *V*-band light curve for comparison (*V* band – grey circles; *J* band – black plus signs; *H* band – grey downward triangles and *K* band – black upward triangles).

A notable feature of the light-curve behaviour is the strong brightening seen at ∼110 d after outburst. This is seen in the *V* band and also *JHK* bands. If the *V*-band brightening was to arise because of destruction of the dust shell, then an increase in the IR fluxes would not be expected. Since this is not the case, the observed behaviour possibly indicates that a second outburst or significant episode of mass loss has taken place at this stage. Such rebrightenings, at late stages, are occasionally known to occur in novae (e.g. V1493 Aql; Venturini et al. 2004) but the cause for it is open to interpretation. The interferometric results (Chesneau et al. 2008) indicate the possibility of a second dust shell forming from the matter ejected in this rebrightening. Though our IR observations could not be continued beyond 126 d after the outburst, the *V*-band photometry shows that V1280 Sco had another phase of rebrightening in October and November 2007 (Munari & Siviero 2007) which lasted for several days. On the whole the object has exhibited a complex light curve.

4 SUMMARY

Near-IR spectroscopy and photometry of the dust forming nova V1280 Sco are presented. The key result concerns the issue of predicting which novae will form dust. Diagnostic lines are identified which are shown to reliably aid in such a prediction. The robustness of the predictive power of these lines can be tested through further observations. A synthetic LTE spectrum is generated to facilitate line identification, to qualitatively study different aspects of the observed spectral features and to give estimates of elemental abundances in V1280 Sco. The presence of a persisting absorption structure in the Br γ line is interpreted as evidence for sustained mass loss during the outburst and used to set a lower limit of 25–27 d for the mass-loss duration. Consistent with the nova's prolonged climb to maximum, it is shown that the actual outburst commenced very early indeed – approximately 13.7 d before maximum light.

ACKNOWLEDGMENTS

The research work at Physical Research Laboratory is funded by the Department of Space, Government of India. We are thankful for the online availability of the Kurucz and NIST atomic line list data base. We also thank the VSNET and VSOLJ, Japan, and AFOEV, France for the use of their optical photometric data. We are grateful to the referee Prof. M. F. Bode for his valuable comments which improved the presentation and contents of the paper.

REFERENCES

Andrea J., Drechsel H., Starrfield S., 1994, A&A, 291, 869
Aller L. H., 1963, The Atmospheres of the Sun and Stars. Ronald Press, New York
Allen C. W., 1976, Astrophysical Quantities. Athlone Press, London and Dover
Ashok N. M., Banerjee D. P. K., 2003, A&A, 409, 1007
Ashok N. M., Banerjee D. P. K., Varricatt W. P., Kamath U. S., 2006, MNRAS, 368, 592
Banerjee D. P. K., Ashok N. M., 2002, A&A, 395, 161
Buil C., 2007, IAU Circ., 8812
Chesneau O. et al., 2008, A&A, 487, 223
Dalgarno A., Stancil P. C., Lepp S., 1997, Ap&SS, 251, 375
Das R. K., Ashok N. M., Banerjee D. P. K., 2007a, CBET, 864
Das R. K., Ashok N. M., Banerjee D. P. K., 2007b, CBET, 866
Das R. K., Ashok N. M., Banerjee D. P. K., 2007c, CBET, 925
della Valle M., Livio M., 1995, ApJ, 452, 704

Evans A., 2001, Ap&SS, 275, 131
Evans A., Geballe T. R., Rawlings J. M. C., Scott A. D., 1996, MNRAS, 282, 1049
Ferland G. J., Lambert D. L., Netzer H., Hall D. N. B., Ridgway S. T., 1979, ApJ, 227, 489
Gehrz R. D., Grasdalen G. L., Hackwell J. A., Ney E. P., 1980, ApJ, 237, 855
Gehrz R. D., Harrison T. E., Ney E. P., Matthews K., Neugebauer G., Elias J., Grasdalen G. L., Hackwell J. A., 1988, ApJ, 329, 894
Gehrz R. D., 1988, ARA&A, 26, 377
Henden A., Munari U., 2007, Inf. Bull. Variable Stars, 5771, 1
Hyland A. R., McGregor P. J., 1989, in Allamandola L. J., Tielens A. G. G. M., eds, Proc. IAU Symp., Vol. 135, Interstellar Dust. NASA CP-3036, NASA, Washington, p. 495
Jose J., Hernanz M., 1998, ApJ, 494, 680
Lynch D. K., Rossano G. S., Rudy R. J., Puetter R. C., 1995, AJ, 110, L2274
Lynch D. K., Rudy R. J., Mazuk S., Puetter R. C., 2000, ApJ, 541, 791
Marshall D. J., Robin A. C., Reyle C., Schultheis M., Picaud S., 2006, A&A, 453, 635
Munari U., Siviero A., 2007, CBET, 1099
Munari U., Valisa P., Della Via G., Dellaporta S., 2007, CBET, 852
Naito H., Narusawa S., 2007, IAU Circ., 8803
Ney E. P., Hatfield B. F., 1978, ApJ, 219, L111
Osborne J. P. et al., 2007, Astron. Telegram, 1011
Prialnik D., Kovetz A., 1995, ApJ, 445, 789
Rawlings J. M. C., 1988, MNRAS, 232, 507
Rudy R. J., 2007, IAU Circ., 8845
Rudy R. J., Dimpfl W. L., Lynch D. K., Mazuk S., Venturini C., Wilson J. C., Puetter R. C., Perry R. B., 2003, ApJ, 596, 1229
Rudy R. J., Lynch D. K., Russell R. W., 2007, IAU Circ., 8809
Sakurai Y., Nakamura Y., 2007, IAU Circ., 8803
Schmeer P., 2007, VSNET-alert 9227
Starrfield S., Gehrz R. D., Truran J. W., 1997, in Bernatowicz T. J., Zinner E., eds, Astrophysical Implications of the Laboratory Study of Presolar Materials. Am. Inst. Phys., New York, p. 203
Swank J., 2007, Astron. Telegram, 1010
Venturini C., Rudy R. J., Lynch D. K., Mazuk S., Puetter R. C., 2004, AJ, 128, 405
Warner B., 2008, in Bode M. F., Evans A., eds, Classical Novae, 2nd edn. Cambridge Univ. Press, Cambridge, p. 21
Wichmann R., Krautter J., Kawara K., Williams R. E., 1990, Astron. Gesellschaft Abstr. Ser., 5, 17
Wichmann R. et al., 1991, in Jaschek C., Andrillat Y., eds, Proc. Int. Coll., Montpellier, France. The Infrared Spectral Region of Stars. Cambridge Univ. Press, Cambridge, p. 353
Williams R. E., 1992, AJ, 104, 725
Yaron O., Prialnik D., Shara M. M., Kovetz A., 2005, ApJ, 623, 398

This paper has been typeset from a TEX/LATEX file prepared by the author.